Technical University of Denmark

DTU

Steam gasification of wheat straw, barley straw, willow and giganteus

Hansen, L.K.; Rathmann, Ole Steen; Olsen, A.; Poulsen, K.

Link back to DTU Orbit

DTU Library
Technical Information Center of Denmark

RISØ

DK9702016

Steam Gasification of Wheat Straw, Barley Straw, Willow and Giganteus

Lars K. Hansen*, Ole Rathmann, Aksel Olsen and Karin Poulsen**

* Present affiliation: FLS Miljø A/S, Ramsingsvej 30, DK-2500 Valby, Denmark
** Present affiliation: ReaTech, CAT Science Centre, Frederiksborgvej 399, P.O. Box 30, DK-4000 Roskilde, Denmark

R ISO-R--944(EN)

Steam Gasification of Wheat Straw, Barley Straw, Willow and Giganteus

Risø-R-944(EN)

Lars K. Hansen*, Ole Rathmann, Aksel Olsen and Karin Poulsen**

* Present affiliation: FLS Miljø A/S, Ramsingsvej 30, DK-2500 Valby, Denmark
** Present affiliation: ReaTech, CAT Science Centre, Frederiksborgvej 399, P.O. Box 30, DK-4000 Roskilde, Denmark

MASTER

Risø National Laboratory, Roskilde, Denmark
August 1997

Abstract A thorough experimental study of the H_2O gasification char-reactivity of wheat straw, barley straw, willow and giganteus at 1-10 bar total pressure, 0.15-1.5 bar H_2O and 0-1.0 bar H_2 and 750-925 C, was performed in a Pressurized Thermogravimetric Analyzer. There were a total of 58 experiments.

Kinetic experiments with char of wheat straw at 10 bar total pressure showed that the reactivity increases with rising temperature and increasing partial pressure of H_2O, while it decreases with increasing partial pressure of H_2. At constant partial H_2O pressure in the absence of H_2, an indication of a negative influence by the total pressure was observed.

Except for the effect of total pressure, the experimental data were analyzed by means of the Langmuir-Hinshelwood equation, including both inhibition by H_2 and reactivity limitation at high H_2O concentration. Also, the reactivity profile was assumed to be independent of temperature and reactant concentration. The value found for the main activation energy E_1, 149 kJ/mole, describing the temperature dependence at low H_2O concentration, is close to experimental values for biomass reported by other workers. At conditions relevant to both fluid-bed and entrained-flow gasifier types the present results indicate an inhibiting effect of the product gas H_2, reducing the reactivity by a factor of up to 10.

A screening study of steam gasification of barley straw, willow and giganteus in addition to the wheat straw showed reaction rates with rather equal temperature dependence. However, at equal temperatures, there was a spread in reactivity of about 10 times from the lowest (wheat and giganteus) to the highest (barley), probably due to different contents of catalytic elements.

DISCLAIMER

Portions of this document may be illegible
in electronic image products. Images are
produced from the best available original
document.

Contents

List of tables

List of figures

1. Introduction

In recent years there has been an increasing interest in pressurized gasification systems due to their potentially high thermal efficiency and reduced environmental impact. The technologies include pressurized fluidized-bed gasification of biomass. In large scale the gasification is typically conducted at 800-1000°C and 10-20 bar in fluid-bed gasifiers and at 1000 - 1800 °C and 20-40 bar in entrained-flow gasifiers. Under these conditions the gasification reaction rate may be controlled by the chemical reaction rate. It is therefore important to know the chemical kinetics when calculating the gasification time for different fuels. The Risø Pressurized Thermogravimetric Analyser (PTGA) has been constructed to investigate gas-solid reaction under pressurized conditions. The pressure can be controlled in the range 1.5-45 bar at maximum 1200°C. During an experiment the weight of the solid sample is measured as a function of time and due to the well-defined conditions in the PTGA, it is very suitable for measuring chemical reactivity. For these kinds of measurements the experimental conditions are chosen so as to ensure constant partial pressures and temperature throughout the entire particle. A thorough description of the PTGA was given by Rathmann (1995). In order to perform measurements under H_2O gasification conditions the flow system of the PTGA was modified slightly as described in Appendix A. By use of the PTGA it is possible to make a systematic test of the influence of different parameters on the chemical reactivity.

It is generally accepted that the reaction of char CO_2 follows a rate law of the Langmuir-Hinshelwood type (Reif, 1952, Alfons and Schoeters, 1985):

$$F(P_{CO_2}, P_{CO}, T) = \frac{k_1 P_{CO_2}}{1 + k_2 P_{CO} + k_3 P_{CO_2}} \qquad (1.1)$$

k_1, k_2 and k_3 are reaction rate constants, P_{CO_2} and P_{CO} are the partial pressures of CO_2 and CO, respectively. This complex rate expression can describe both reactivity limitation at high reactant concentration (k_3) and inhibition by the product gas (k_2).

In several works CO_2 gasification of coal in PTGA have been studied as well as biomass. The range of the activation energy (E_1) from 10 different works was found to be between 100 and 193 kJ/mole and with an average value of 157 kJ/mole (Gjernes et al., 1995). Illerup and Rathmann, 1996 found an activation energy of 152 kJ/mole for wheat straw.

In the present work a thorough investigation of the H_2O gasification kinetics of wheat straw is given, using a similar Langmuir-Hinshelwood rate law equation.

$$F(P_{H_2O}, P_{H_2}, T) = \frac{k_1 P_{H_2O}}{1 + k_2 P_{H_2} + k_3 P_{H_2O}} \qquad (1.2)$$

The experiments were carried out at 10 bar and at 650-925°C. The pulverized straw has been pyrolyzed in the Risø Pressurized Entrained-flow Reactor (PEFR) at 15 bar and 900°C. The PEFR is described by Hansen et. al. (1995). The influence of the gasification pressure in the PTGA was tested in the range 1-10 bar. Screening tests with barley straw, willow and giganteus have been conducted at 10 bar.

2. Experiments

2.1 Experimental conditions

The experiments have been carried out in the pressurized thermogravimetric analyzer with four different biomasses prepyrolyzed in the pressurized entrained-flow reactor (PEFR) at Risø.

Kinetics:

The wheat straw sample, used for the kinetic experiments, consisted of straw ground to a particle size < 150 μm and pyrolyzed in the PEFR at 900°C and 15 bar. The experimental conditions in Table 2.1 were chosen in order to determine the kinetic parameters given in equations 2.1 and 2.2. The rate of reaction, $F(P_{reactant}, P_{product}, T)$, is expressed by the Langmuir-Hinshelwood expression:

$$F(P_{H_2O}, P_{H_2}, T) = \frac{k_1 P_{H_2O}}{1 + k_2 P_{H_2} + k_3 P_{H_2O}} \qquad (2.1)$$

The rate constants are described by an Arrhenius equation:

$$k_i = k_{0i} e^{\frac{-E_{oi}}{RT}} \qquad (2.2)$$

In the present work 24 kinetic experiments have been carried out (Appendix B). The temperature range was chosen so as to obtain a rate of reaction controlled by the chemical reaction and a time for complete conversion that was not too long. The partial pressures of the reactant and product gases in Table 2.1 were chosen to cover the range of interest for industrial gasifiers as well as possible. The experiments in the PTGA have been carried out at 10 bar and with a gas flow of 4-6 Nl/minute corresponding to a superficial velocity of 2-3 cm/s in the reaction chamber.

Table 2.1. Wheat char gasification conditions for kinetic experiments.

Particle size	< 150	μm
Pyrolysis temperature	900	°C
Pyrolysis pressure	15	bar
Pyrolysis time	2 - 3	s
Gasification temperature	750-925	°C
Gasification pressure	10	bar
Partial pressure of H_2O	0.35-1.5	bar
Partial pressure of H_2	0-1.5	bar

The influence of the total pressure has been investigated under the conditions listed in Table 2.2.

Table 2.2. Wheat char gasification conditions for total-pressure experiments.

Particle size	< 150	μm
Pyrolysis temperature	900	°C
Pyrolysis pressure	15	bar
Pyrolysis time	2 - 3	s
Gasification temperature	750-900	°C
Gasification pressure	1-10	bar
Partial pressure of H_2O	0.15-0.75	bar

2.2 Experimental procedure

Approximately 7 mg of the fuel sample was placed on the sample tray, the pressure vessel was closed and the vessel pressurized. All gas lines carrying steam containing gases were kept at 250-290°C, a temperature well above the water boiling point at the experimental pressure. In advance of the actual experiment the steam generator was producing steam at the chosen experimental conditions (rate and pressure) to a pressurized bypass line in order to give a steam flow rate variation as small as possible at the moment when the steam was switched on to the test gas inlet line.

The sample was heated to 150°C in N_2 for 15 minutes and the weight of the dry sample was measured. After drying the temperature was raised to the reaction temperature and the sample was kept at this temperature for about 5 minutes before the steam and hydrogen were supplied. By the end of each experiment, the temperature was raised to 1000°C to force complete conversion in order to measure the ash weight. An example of a method-file containing the set points are given in Figure 2.1. Figure 2.2 shows the temperature and weight as a function of time for a typical experiment.

```
Method file: c:\ptga\methods\HH20.96\HH20#21.MET

Description: H20 3.5%, 10bar, 850gr., Wheat char#1

Log file: * = c:\PTGA\METHODS\HH20.96\HH20#21.LOG

No. of lines:   11
```

line #	Dur.min	Rate d/m	Temp.	stat	RFlow	DFlow	Press
1	2	0	26	1	500	100	10
2	1	0	200	1	500	100	10
3	15	0	200	1	2000	300	10
4	20	0	200	1	5700	1200	10
5	21.67	30	850	1	5700	1200	10
6	15	0	850	1	5500	1200	10
7	90	0	850	3	5500	1200	10
8	5	30	1000	3	5500	1200	10
9	7	0	1000	3	5500	1200	10
10	5	0	800	1	5700	1200	10
11	30	0	20	1	2000	300	10
Total	211.67						

Figure 2.1. Method-file containing set-points.
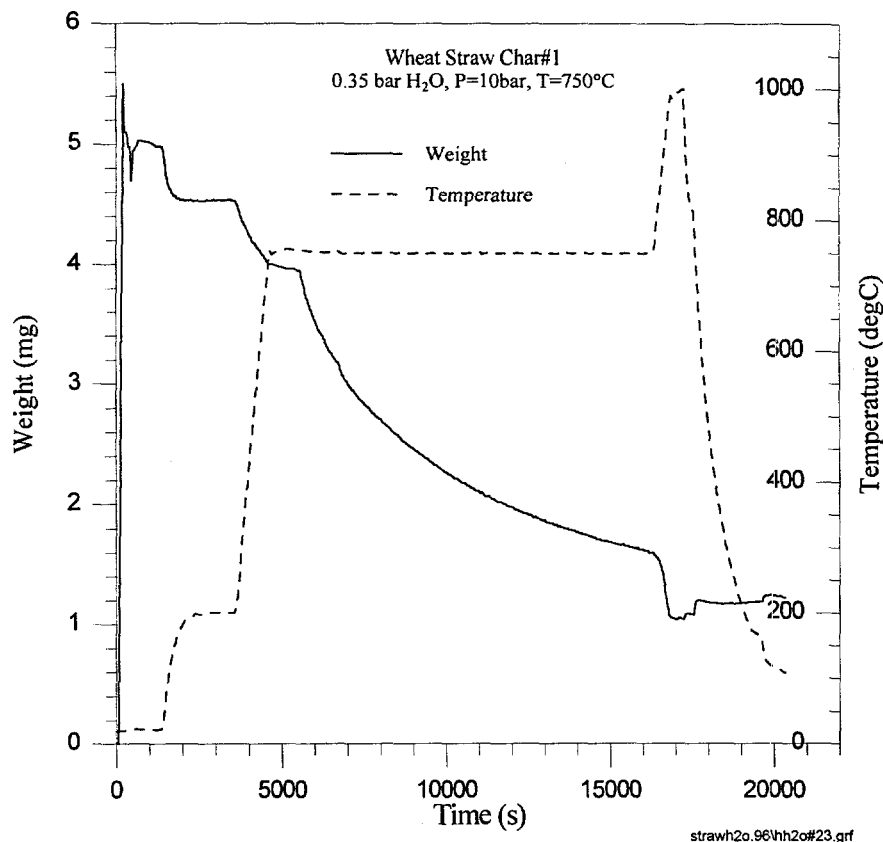
Figure 2.2. Temperature and weight as a function of time.

2.3 Analysis of experimental results

The weight signal was converted from millivolt to milligram and compensated for the effect of thermal expansion of the balance arm of the PTGA and of the buoyancy (Rathmann, 1995). A special program was used in order to calculate the conversion and reactivity based on equations 2.3 and 2.4, respectively.

$$X = 1 - \frac{m - m_{ash}}{m_0 - m_{ash}} \qquad (2.3)$$

$$R_n = -\left(\frac{1}{m - m_{ash}}\right)\frac{dm}{dt} \qquad (2.4)$$

where m is the mass as a function of time, t is the time, m_0 is the mass of the sample at the beginning of an experiment and m_{ash} is the mass of the ash in the sample. The derivative in the right-hand side of equation 2.4 was found by a numerical scheme, which also included averaging over a number of subsequent single measurements for the purpose of noise rejection.

The average value of the observed reaction rate was preferably calculated over the conversion range of 40 - 60% for use in the further analysis. Figure 2.3 gives an example of a reactivity plot. With the presence of H_2 in the experiments this averaging range had to be displaced to higher conversion values due to a longer dead time in the H_2 line compared to the steam line.

Figure 2.3. Reactivity of wheat char at 1.5 bar H_2O, 0 bar H_2, 750 °C and 10 bar.
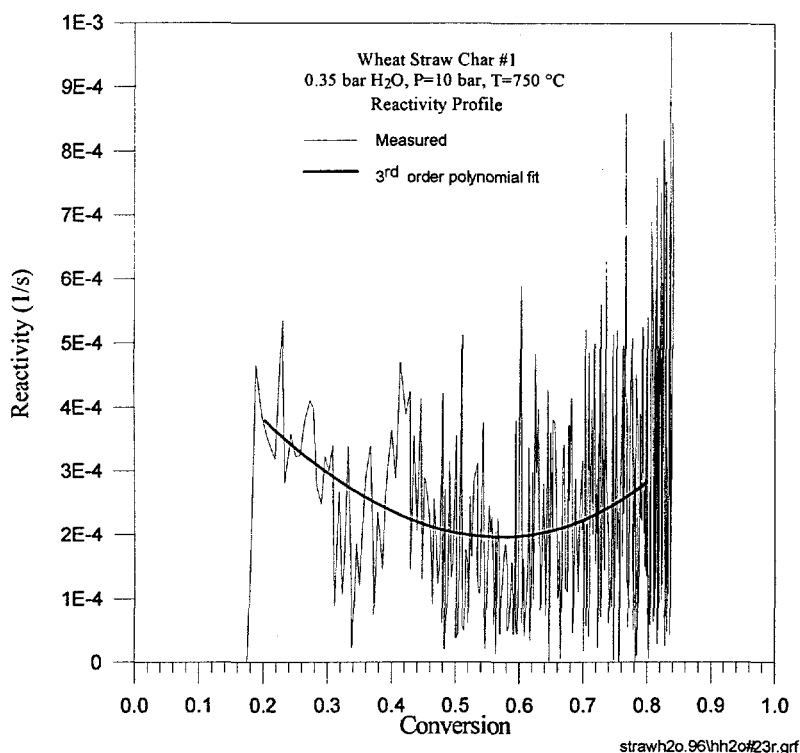
The reactivity program also calculated the maximum rate of diffusion of reactant gas to the particles in order to ensure that the reaction was truly based on the kinetic reactivity and not limited by diffusion. The ratio between maximum diffusion rate and reactivity was always in the range 10-1000. Thus, the reaction rate was always safely within the kinetic regime.

3. Experimental results

This chapter describes the H_2O gasification of biomass char carried out with gases containing H_2O, H_2 and N_2. In section 3.1 the kinetic parameters for H_2O gasification of wheat straw are derived according to equation 2.1. In section 3.2 the influence of total pressure on the reactivity of wheat straw is described. The results of comparing the reactivities of wheat, barley, willow and giganteus are reported in section 3.3.

3.1 Kinetic parameters for wheat straw

The experiments were carried out under the experimental conditions given in Appendix B. Figure 3.1 shows the reactivity as a function of the temperature for the experiments carried out with different pressures of H_2O in the absence of H_2 and a total pressure of 10 bar. As expected the reactivity increases with increasing temperature and increasing partial pressure of H_2O. However, the effect of reactivity limitation at high H_2O concentration is visible in the whole H_2O range as the reactivity increases less than in proportion to the partial pressure.
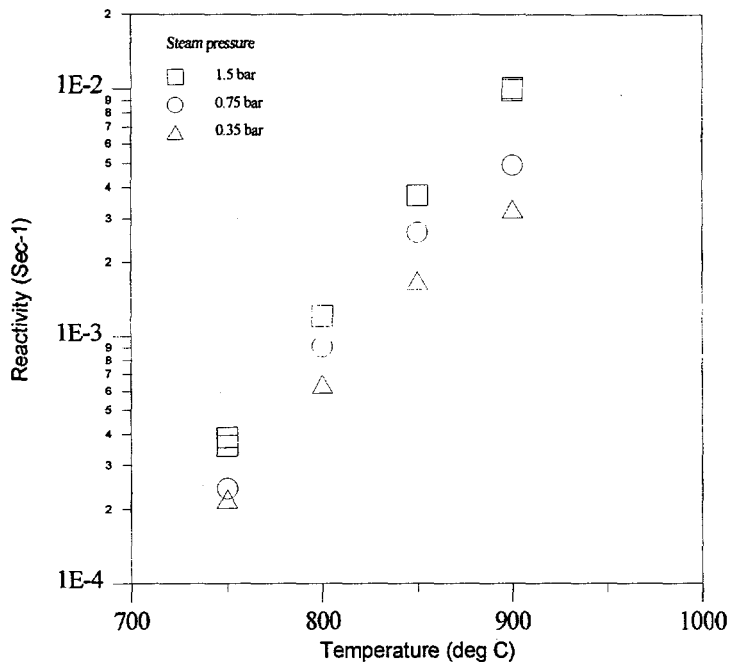
Figure 3.1. Gasification of wheat char 0.35-1.5 bar H_2O, 0 bar H_2 at 10 bar total pressure.

Equation 3.1. shows that on plotting $1/R_n$ as a function of $1/P_{H_2O}$ at equal temperatures, k_1 and k_3 can be found from the slope and the Y-axis interception of a fitting line. This is illustrated in Figure 3.2 showing the graphs for 750, 800, 850 and 900°C. It is seen that straight lines give a good representation of the experimental results, which means that the relation between the rate of reaction and the H_2O partial pressure can be described by equation 3.1 when the partial pressure of H_2 is zero.

$$R_n = \frac{k_1 P_{H_2O}}{1 + k_3 P_{H_2O}} \qquad \Leftrightarrow \qquad \frac{1}{R_n} = \frac{1}{k_1} \cdot \frac{1}{P_{H_2O}} + \frac{k_3}{k_1} \qquad (3.1)$$
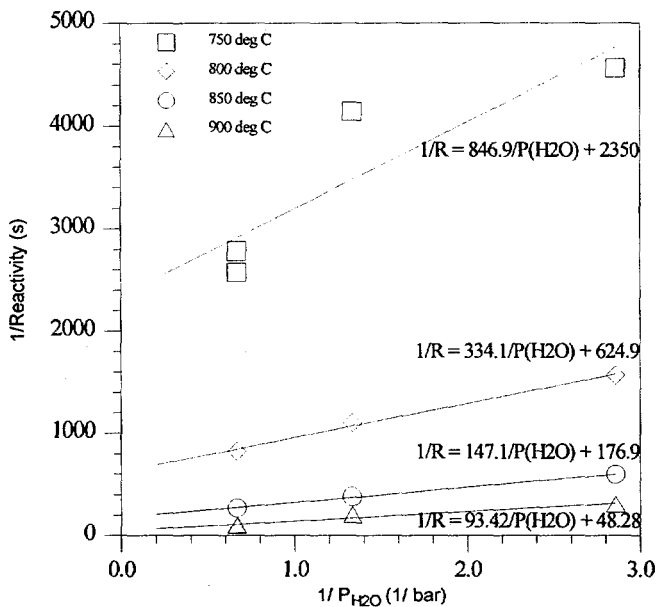
Figure 3.2. Inverse reactivity for H_2O gasification of wheat char.

The temperature dependence of k_1 and k_3 is found from Figure 3.2 and is listed in Table 3.1.

Table 3.1. Experimental values of k_1 and k_3 at 750, 800, 850 and 900 °C.

Temperature (°C)	1/T (1/K)	k_1 (1/s bar)	k_3 (1/bar)
750	0.0009775	0.000118	2.775
800	0.0009320	0.002993	1.870
850	0.0008905	0.006798	1.203
900	0.0008525	0.010704	0.517

From Figures 3.3 and 3.4 it is seen that the Arrhenius equation (2.2) describes the temperature dependency quite well for both k_1 and k_3. The actual Arrhenius expressions with best-fit pre-exponential factors and activation energies are given in equations (3.2) and (3.3).
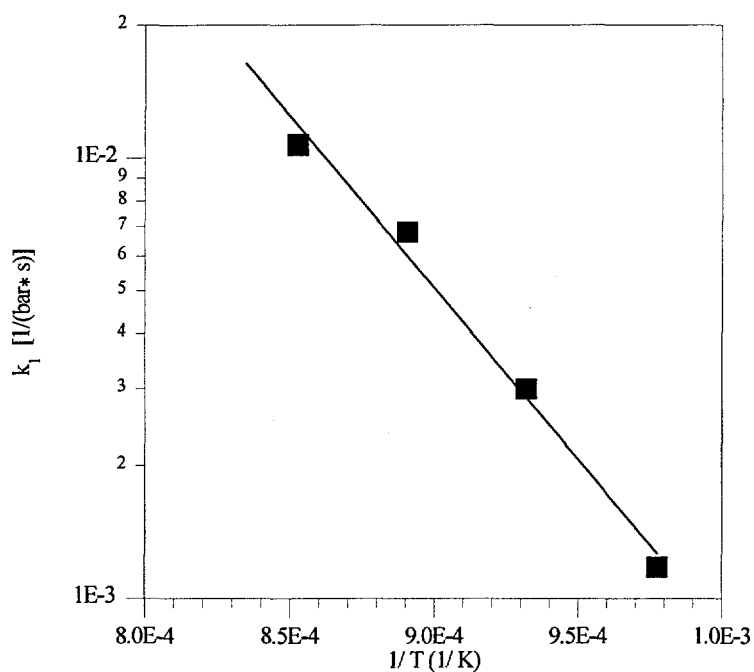
Figure 3.3. Arrhenius plot for k_1.
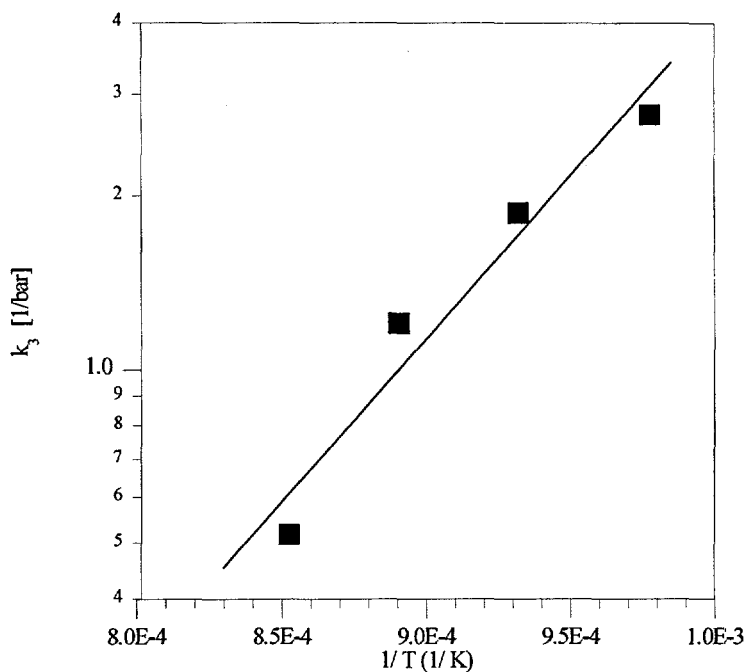
Figure 3.4. Arrhenius plot for k3.

$$k_1 = 51.3 \cdot 10^3 \cdot e^{\frac{-149 \cdot 10^3}{RT}} \qquad \textbf{(3.2)}$$

$$k_3 = 9.10 \cdot 10^{-6} \cdot e^{\frac{+108 \cdot 10^3}{RT}} \qquad \textbf{(3.3)}$$

The activation energy for k_1 is found to be 149 kJ/mole while the pseudo-activation energy associated with k_3 is found to be negative (-108 kJ/mole). This reflects the fact that the limitation effect decreases with increasing temperature and that the effect is negligible at high temperatures. In figure 3.5 it is shown that, using the deduced expressions for k_1 and k_2, the experimental reactivity data are well represented by the Langmuir-Hinshelwood law.
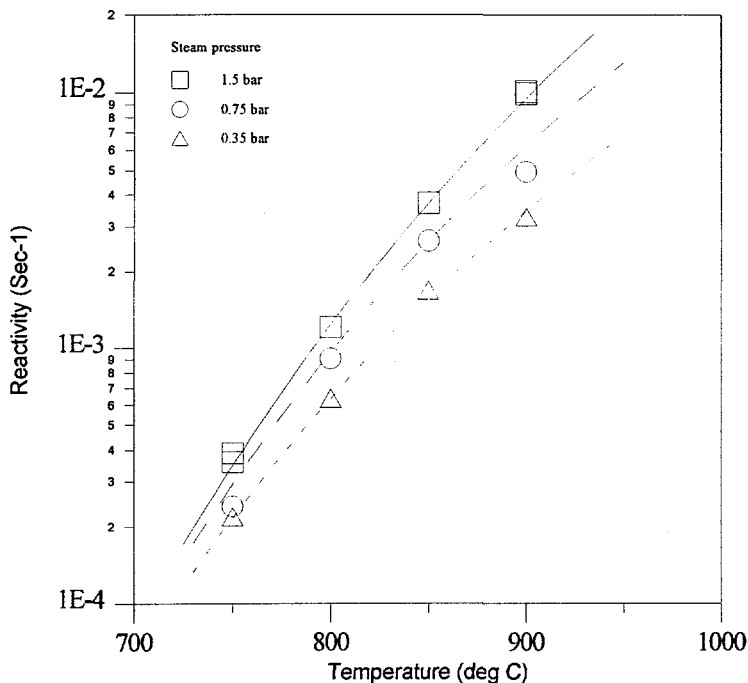
Figure 3.5. Gasification of wheat char 0.35-1.5 bar H_2O, 0 bar H_2, 10 bar. Experimental data and the Langmuir-Hinshelwood law.

The above results may be compared with the results reported by Moilanen et al. (1993) for steam gasification of peat and brown coal. Assuming the gasification to be a 1st order process, they found activation energies ranging from 194 to 267 kJ/mole. Consequently, their activation energies include to some extent also the effect of reactivity limitation. Depending on whether far from or close to reactivity limitation, the corresponding 1st order activation energy of the present study would be a value somewhere between $E_1 =$ 149 kJ/mole and E_1-E_3 = 257 kJ/mole, and actually this range overlap well with the results of Moilanen et al. The present activation energy is also close to the value of 152 kJ/mole found by Illerup and Rathmann (1996) for CO_2 gasification.

For coal, activation energies from 188 to 272 kJ/mole can be found in the review by Laurendeau (1978), while a more recent study by Mühlen et al. (1985) reports a value of 154 kJ/mole. Mühlen also reports the corresponding activation energy for CO_2 gasification, 153 kJ/mole, very close to that. Thus the activation energy for steam gasification of biomass char seems to be a little lower than for coal char. This may possibly be due to the higher content of catalysts in biomass (alkali metals), the effect of which is reduced with increasing temperature.

Figure 3.6 shows the reactivity for the experiments carried out with a mixture of 1.5 bar H_2O and 0, 0.5 and 1.0 bar H_2. When the reactant gas contains H_2 the rate of reaction is much slower than that for a gas containing only H_2O. The experiments are therefore carried out at a higher temperature level 800-925°C in order to obtain reasonable reaction rates.
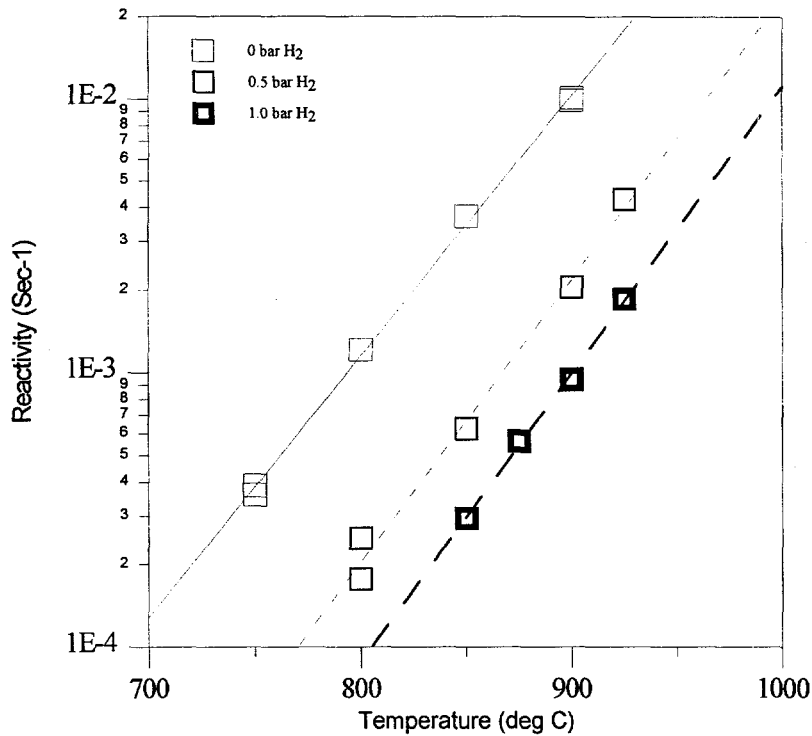
Figure 3.6. Gasification of wheat char 1.5 bar H_2O, 0-1 bar H_2 and 10 bar total pressure. The trend of the experimental data is indicated by straight lines.

From the experiments shown in Figure 3.6, k_2 can be deduced by means of equation 1.2 for 800, 850 and 900°C using the values for k_1 and k_3 found from equations 3.2 and 3.3, as shown in Figure 3.7.
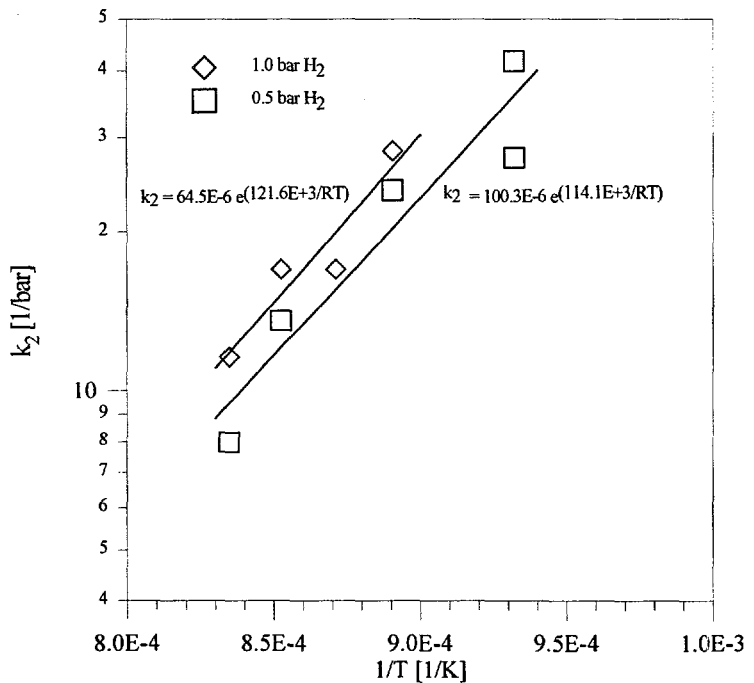
Figure 3.7. Arrhenius plot of k_2.

Despite the large uncertainty of k_2, the plot in Fig. 3.7 shows that the temperature dependency is fairly well described by an Arrhenius law. However, the scaling factor

differs a little between the 1.0 and the 0.5 bar H_2 experiments, while there is only little difference in slope. For the further analysis the geometrical mean of the two expressions is used as shown in equation 3.4.

$$k_2 = 80.4 \cdot 10^{-6} \cdot e^{\frac{+117.9 \cdot 10^3}{RT}} \qquad (3.4)$$

As for k_3, k_2 decreases with increasing temperature, meaning that the inhibiting effect of the product gas, H_2, decreases with increasing temperature.

Values for k_2, calculated from equation 3.4, are listed in Table 3.2.

Table 3.2. Calculated values of k_2 (best-fit parameters).

| Temp. (°C)	1/T (1/K)	k_1 (1/s bar)	k_3 (1/bar)	k_2 (1/bar)
750	0.0009775	0.001263	3.0999	79.0
800	0.0009320	0.002854	1.7133	41.5
850	0.0008905	0.006005	0.9976	23.1
875	0.0008708	0.008548	0.7717	17.6
900	0.0008525	0.011867	0.6080	13.5
925	0.0008347	0.016326	0.4821	10.5
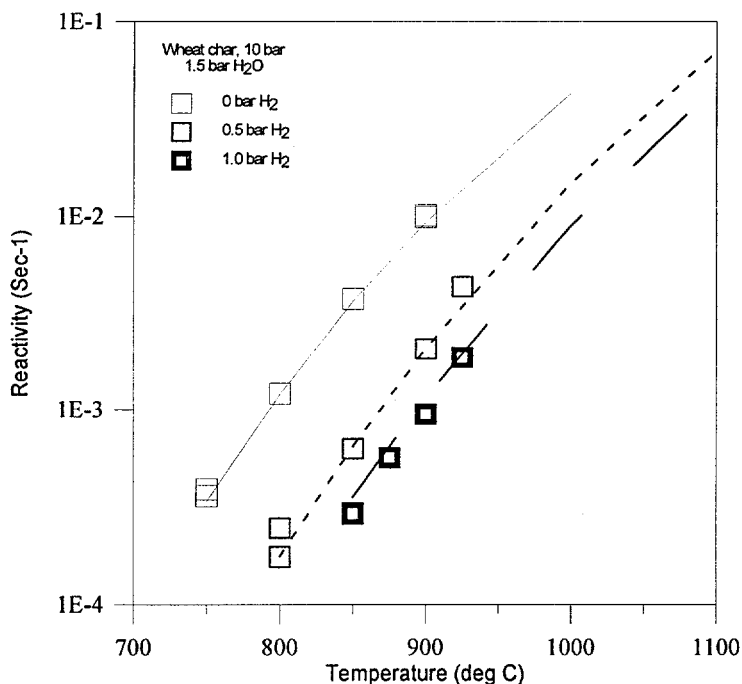
Figure 3.8. H_2O/H_2 gasification of wheat char. Experimental data and the Langmuir-Hinshelwood law

As seen from Figures 3.8 and 3.5 the Langmuir-Hinshelwood rate law represents the experimental data accurately, with respect to the effect on the reactivity of both temperature and partial pressure of H_2O and H_2. Both reactivity limitation and inhibition effects decrease with increasing temperature reflected by the negative pseudo-activation energies of k_2 and k_3. The inhibiting effect of the product gas H_2 at 1 bar partial pressure is seen to be quite significant by decreasing the reactivity by one order of magnitude at 850°C, relevant for fluid-bed applications. For entrained-flow reactors operating with higher partial pressures of H_2 (5 bar) the inhibiting effect will presumably be significant at temperatures as high as 1500°C, which is also illustrated in figure 3.8.

3.2 Influence of total pressure

The influence of total gasification pressure at constant H_2O partial pressure has been investigated at 1-10 bar total pressure and 0.15-0.75 bar H_2O in the absence of H_2. In Figures 3.9 to 3.11 the reactivity as a function of temperature is seen for H_2O partial pressures 0.75, 0.35 and 0.15 bar. For experimental reasons not all combinations of total pressure and H_2O were possible

Figure 3.9. Gasification of wheat char at 0.75 bar H_2O partial pressure.

Figure 3.10. Gasification of wheat char at 0.35 bar H_2O partial pressure.

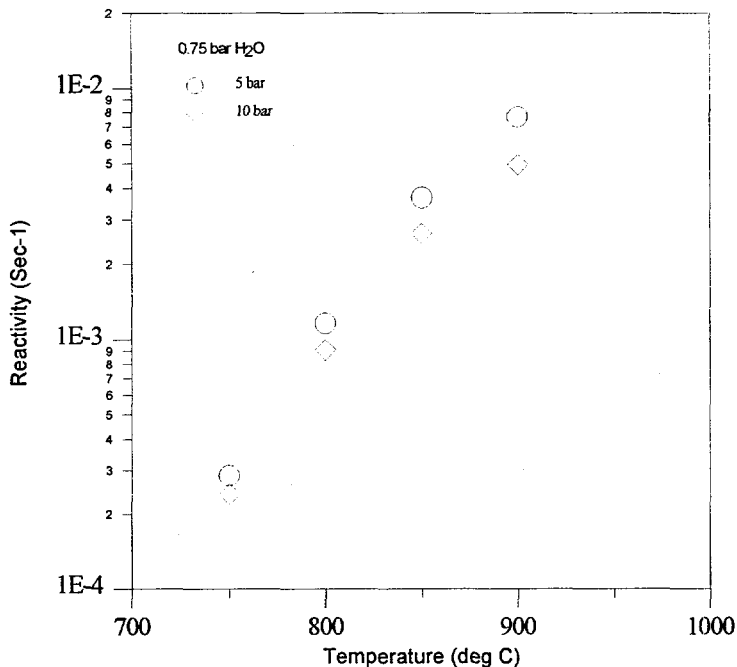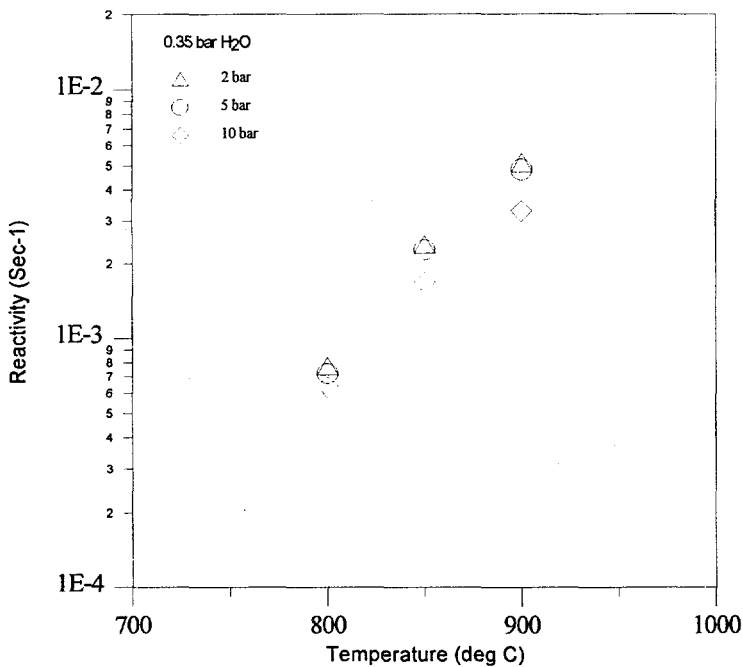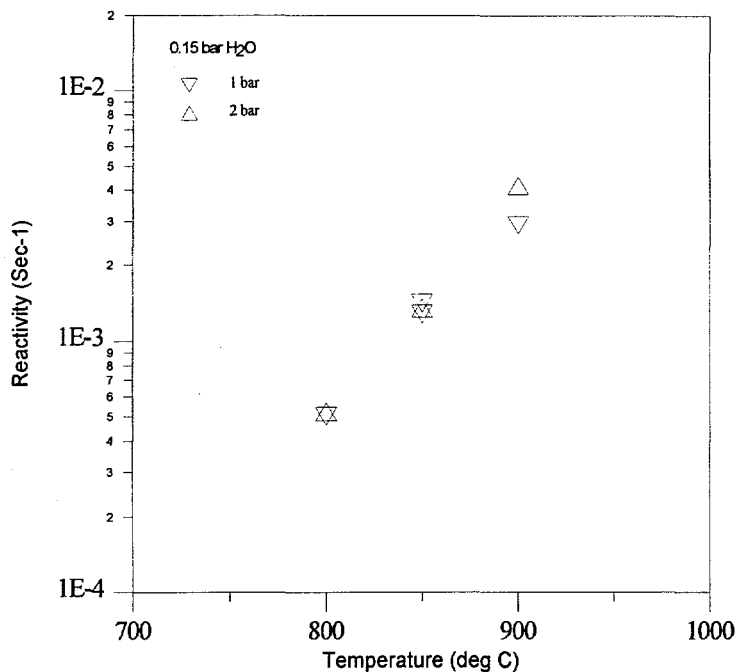*Figure 3.11. Gasification reactivity of wheat char at 0.15 bar H₂O partial pressure.*

At 0.75 and 0.35 bar H_2O (figures 3.9 and 3.10) there seems to be a negative influence on the reactivity of increased total pressure from 5 to 10 bar: a decrease of 20% at 750-800°C and more than 50% at 900°C. At a H_2O partial pressure of 0.15 bar there is no significant difference between 1 and 2 bar. At these low H_2O pressure tests the steam generator was operating at the very low side of its capacity range, and instabilities of the steam production rate may have occurred.

A similar effect was also observed for CO_2 gasification (Illerup and Rathmann, 1996). However, these experimental series are not sufficiently accurate to conclude whether the influence of total pressure is a real physical-chemical effect. Thus, a temperature post-calibration of the PTGA performed by Sørensen (1997) showed that the (small) temperature difference between the measuring thermocouple and the sample is affected by the total pressure, and that this, in turn, could explain part of the apparent pressure effect on the reactivity. From the 0.15 bar H_2O gasification measurements no clear conclusion can be drawn regarding the total pressure behaviour due to the uncertainty of a stable steam supply.

3.3 Screening of different biomasses

The influence of fuel type on the gasification rate has been tested with four different types of biomasses: wheat straw, barley straw, willow and elephant grass. The experimental conditions are given in Table 3.3.

Table 3.3. Gasification of wheat, barley, willow and giganteus with H₂O.

Particle size	< 150	µm
Pyrolysis temperature	900	°C
Pyrolysis pressure	15	bar
Pyrolysis time	2 - 3	s
Gasification temperature	650-850	°C
Gasification pressure	10	bar
Partial pressure of H_2O	1.5	bar
Partial pressure of H_2	0	bar

The screening tests are listed completely in Appendix B.

The different kinds of biomasses have been compared with respect to the H_2O reactivity in the absence of H_2. Figure 3.12 shows the reactivity as a function of temperature for the experiments carried out with 1.5 bar H_2O. The reactivity for the barley straw is nearly 10 times higher than that for wheat straw and giganteus, and 5 times higher than that found for willow. The ranking of the different biomass types are the same as for CO_2 gasification as reported by Illerup and Rathmann, (1996).
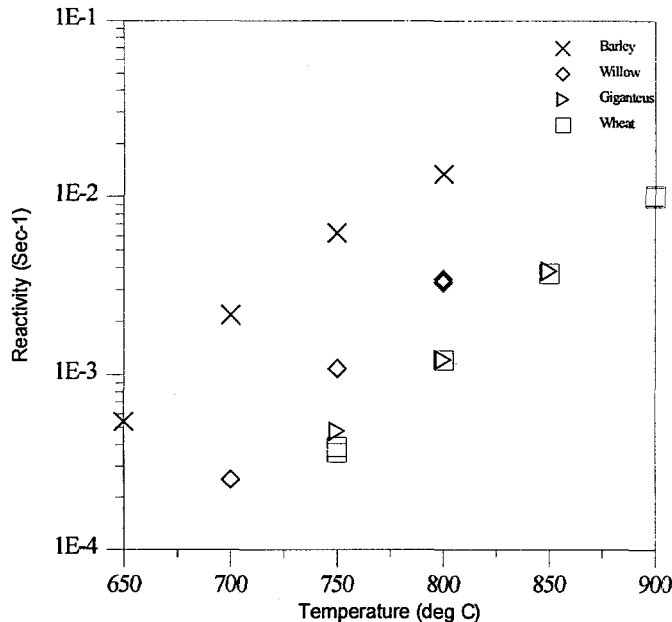

Figure 3.12. Comparison of gasification reactivities of four different biomass fuels.

As seen from Appendix D the variation in the ash composition is large for the four biomasses. Especially in the content of potassium the barley straw has a much higher value than the other biomasses. It is well established that potassium catalyzes the reaction between H_2O and char, which may explain the much higher reactivity rate of barley.

4. Conclusion

A thorough experimental study of the H_2O gasification char-reactivity of wheat straw, barley straw, willow, giganteus at 1-10 bar total pressure, 0.15-1.5 bar H_2O and 0-1.0 bar H_2 and 750-925°C, was performed in a Pressurized Thermogravimetric Analyzer.

Kinetic experiments with char of wheat straw at 10 bar total pressure showed that the reactivity increases with increasing temperature and increasing partial pressure of H_2O. However, the effect of reactivity limitation at high H_2O concentration is visible in the whole H_2O range as the reactivity varies less than in proportion to the partial pressure of H_2O. In the experiments with different contents of H_2 in the reaction gas a large inhibiting effect on the reactivity by H_2 was observed. Both the reactivity limitation and inhibition effects were observed to decrease clearly with increasing temperature.

The experimental data for wheat straw char kinetics at 10 bar are very well described by the Langmuir-Hinselwood equation including both inhibition with H_2 and reactivity limitation at high H_2O concentration. The value of the main activation energy $E_1 = 149$ kJ/mole, describing the temperature dependence at low H_2O concentration, is close to the experimental values reported by other workers for biomass and coal, and is about the same as found in a previous study of CO_2 gasification.

Experiments at varying total pressure and constant H_2O partial pressure in the absence of H_2 indicated a negative influence on the reactivity by the total pressure, not accounted for by the Langmuir-Hinshelwood rate law. Post-calibration of the experimental equipment by Sørenesen (1997) showed that for some part this observation can be explained by a pressure dependent temperature defect in the control of the sample temperature. More detailed studies will be necessary to give evidence for such a total pressure effect.

A screening study for all four biomass types at 10 bar total pressure, 1.5 bar H_2O, no H_2 and 650-900°C showed that while the temperature dependences were rather equal the absolute reaction rate had a spread of 10 times from wheat and giganteus as the lowest to barley as the highest. Chemical analyses of the biomasses show that the variation in the content of H, C and N is small while the ash composition as well as the fusion temperatures are very different. Especially the content of potassium has a much higher value in barley straw than in the other biomasses. This may explain why barley straw has the highest reactivity.

For both fluid-bed and entrained-flow gasifier types the present experimental study indicates that the inhibiting effect of the product gas H_2 is of significant importance, decreasing the reactivity by roughly one order of magnitude at relevant product gas partial pressures.

5. Acknowledgement

6. References

Gjernes, E., Fjellerup, J., Hansen, L. K., Rathmann, O., Kirkegaard, M., Bak, J., Stoholm, P., Illerup, J. B., Hald, P. and Olsen, A., 1995, *Theoretical and Experimental Investigations of coal and biomass combustion and gasification properties at high pressure and temperature - Final Report. Risø-R-859(EN)*, Risø National Laboratory, Denmark.

Hansen, L. K., Fjellerup, J., Stoholm, P. and Kirkegaard. M., 1995, *The pressurized Entrained Flow Reactor at Risø. Design Report Risø-R-822(EN)*, Risø National Laboratory, Denmark.

Illerup, J. B. and Rathmann, O, 1996, *CO$_2$ Gasification of Wheat Straw, Barley Straw, Willow and Giganteus. Risø-R-873(EN)*, Risø National Laboratory, Denmark.

Laurendeau, N.M. (1978). *Heterogeneous Kinetics of Coal Char Gasification and Combustion.* Prog.Energy Combust. Sci. **4**, pp 221-270.

Mühlen, H.-J., van Heek, K.H. and Jüntgen, H. (1985). *Kinetic studies of char in the presence of H$_2$, CO$_2$ and CO.* Fuel **64**, pp 944-949.

Moilanen,A., Saviharju,K. and Harju,T. (1993*). Steam gasification reactivities of various fuel chars,* in: Advances in Thermochemical Biomass Conversion, pp.131-141, edited by Bridgwater, A.V., Blackie Academic & Professional (1993).

Overend, R. P., Milne, T. A. and Mudge, L. K. (1985). *Fundamentals of Thermochemical Biomass Conversion*, Elsevier Applied Science Publishers LTD, 619-689.

Rathmann, O., Stoholm, P. and Kirkegaard, M. (1995). *The Pressurized Thermo-gravimetric Analyzer at the Department of Combustion Research, Risø: Technical Description of the Instrument.* Risø-R-823(EN), Risø National Laboratory, Denmark.

Reif, A. E. (1952). *The mechanism of the carbon dioxide-carbon reaction,* J. Phys. Chem., **56**, 785.

Sørensen, L.H., ReaTech, CAT Science Center, Frederiksborgvej 399, P.O.Box 30, DK-4000 Roskilde, Denmark. *Private communication* (1997).

7. Appendices

Appendix A

Modification of the Risø PTGA: Establishment of Forced Purge Flow into the Balance Unit.

Ole Rathmann

INTRODUCTION

Originally, the Risø PTGA used a flow configuration as described by Rathmann et al. (1995), where the purge flow through the balance unit was obtained indirectly by suction from the pressure vessel volume by the difference between the specified exit flow and the somewhat smaller specified test gas inlet flow. The advantage of this configuration is the vanishing pressure difference between the pressure vessel volume on the one hand and the balance unit housing, reaction chamber and connected gas flow lines on the other. Thereby complete tightness between the last-mentioned components in the pressure vessel is not so critical. However, the purge flow gets extremely sensitive to fluctuations in the inlet test gas flow, e.g. due to instabilities in steam generator operation during steam gasification experiments.

During steam gasification tests with this original flow configuration condensation in the balance unit was impossible to avoid, and the weight signals were spoiled due to droplets clinging to the balance arm. The reason is believed to be short-period flow reversals in the purge flow, due to fluctuations in the generated steam flow from the steam generator, as explained above.

As a consequence, the flow configuration has been changed, so that the purge flow is forced through the balance unit by a direct connection between a mass flow controller and the balance unit housing. This should to a much higher degree ensure a positive purge flow to prevent the reaction test gas containing H_2O from entering the balance unit housing to cause condensation.

DESCRIPTION OF CONFIGURATION B.

The new configuration is shown in Fig. 1.1 and Fig. 1.2.

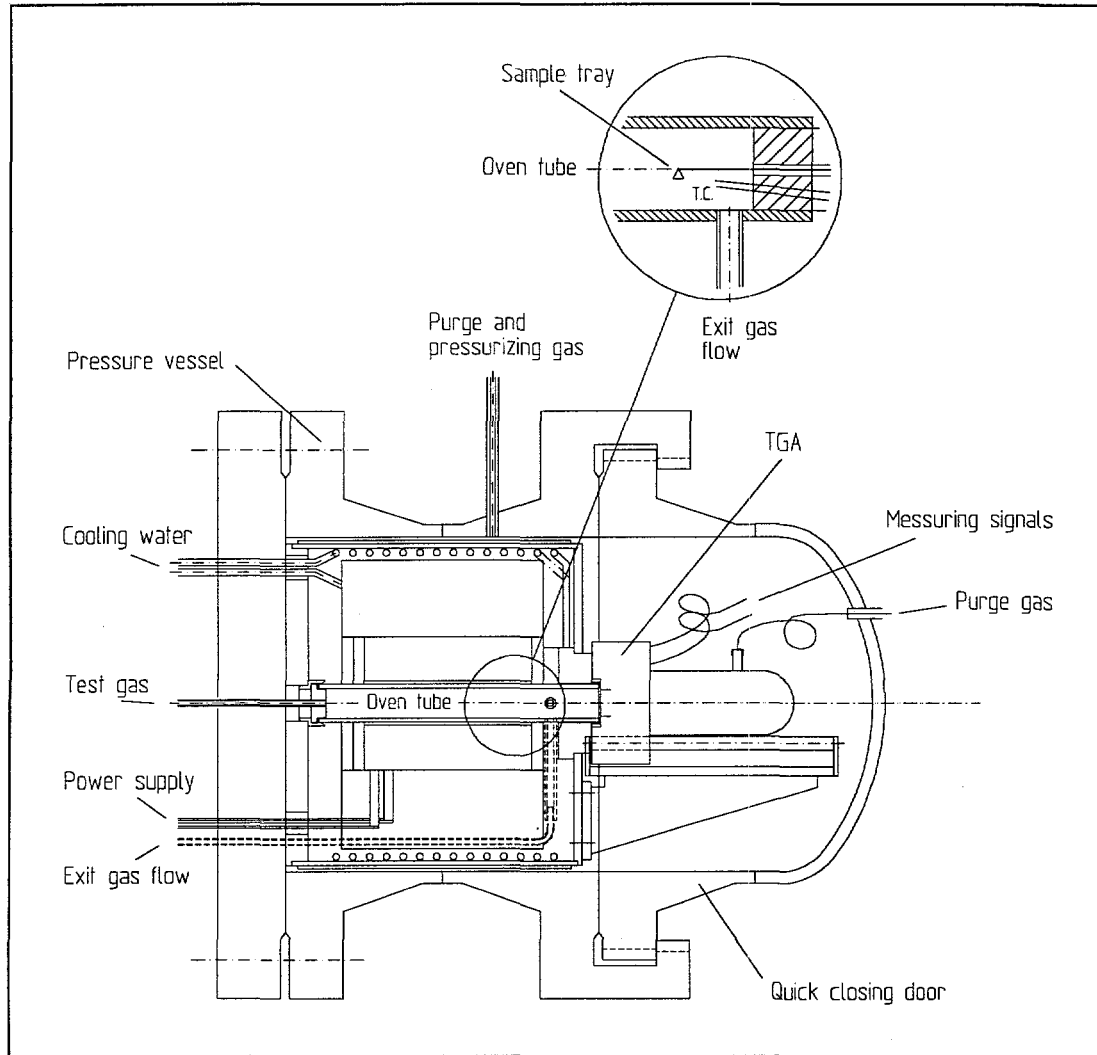*Fig. 1.1. Pressure vessel with furnace and balance unit.*

The physical connection for the purge gas flow from the mass flow controller to the balance housing is established through a feed-through placed in the quick-closing door of the pressure vessel as shown in Fig. 1.1.

Symbols:

(symbol)	Solenoid valve.
(symbol)	Safety valve.
(symbol)	Flow controller/meter. (Valve)
(symbol)	Orifice flow restriction.
(symbol)	Power supply.
D/A A/D	Digital/Analog conversion unit.
BCU	Balance Control Unit.
- - - -	Electrical/Signal connection.
(PT)	Pressure transmitter.
(symbol)	Condensing water trap.
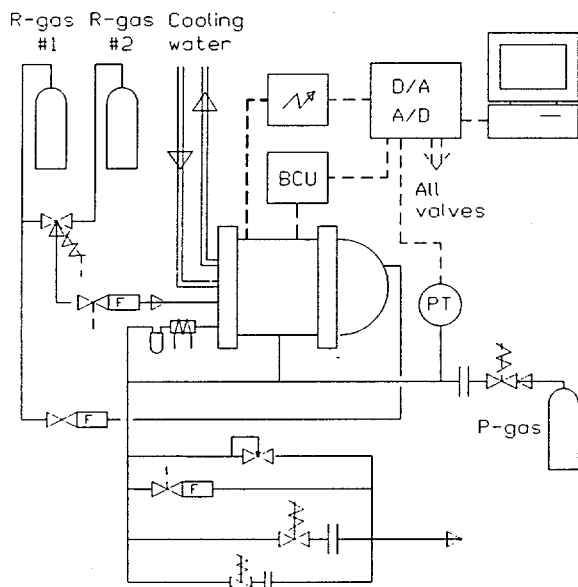
Fig. 1.2. PTGA System layout.

R-gas #1 and #2: Selectable 'reaction' test gases. R-gas #1 is normally inert (N_2) and is also used as purge gas.

P-gas: Pressurizing gas.

In the case of steam gasification experiments, steam is added from a steam generator into the reaction gas flow line between the mass flow controller and the centre of the back wall (left) of the pressure vessel.

The two solenoid pressure relief valves in connection with flow limiting orifices, seen in the bottom of the figure, differ from each other in that the upper one, with the larger orifice (FDV), is of the normally-closed type, and is used for normal pressure blow-down, while the lower one with the smaller orifice (SDV) is of the normally-open type and is used to relieve the pressure in case of such abnormal situations as overpressure, overtemperature or electrical power fall-out.

Fig. 1.2 shows the modified flow path configuration. This configuration is similar to that used by Dobner et al. (1976). Following a condensing water trap outside the vessel the exit flow is led to a pressure balance line connected to the pressure vessel volume. Pressurization and depressurization (through solenoid valves in connection

with flow- limiting orifices) and pressure control during constant pressure conditions (by a mass flow controller) take place via this pressure balance line.

Due to the pressure drop through the narrow exit gas flow lines at some places the 'internal components' - the balance unit housing and the reaction chamber tube and connected flow lines - will be at a certain overpressure relative to the pressure vessel volume. Preliminary tests indicates overpressures of about 10-30 mbar at operation at 20 bar. This means that the tightness of the fittings between these 'internal components' is important to avoid humid gas to leak out into the pressure vessel volume, where it may condense and thereby damage the insulation material of the furnace. Special attention has been given to the fittings between the reaction tube and the balance housing and the steel capillary tube exit flow line. The fitting between reaction tube and the balance housing is sealed with a rubber gasket, while the fitting between the exit flow branch of the reaction tube (quartz) and the steel capillary tube is made with a ceramic tube with teflon tape as the sealing material as shown in Fig. 1.3. The tightness of these fittings have been tested at atmospheric pressure at realistic overpressures, temperatures and flow rates, and it was found that the leakage's were less than 1% of the exit flow rate.
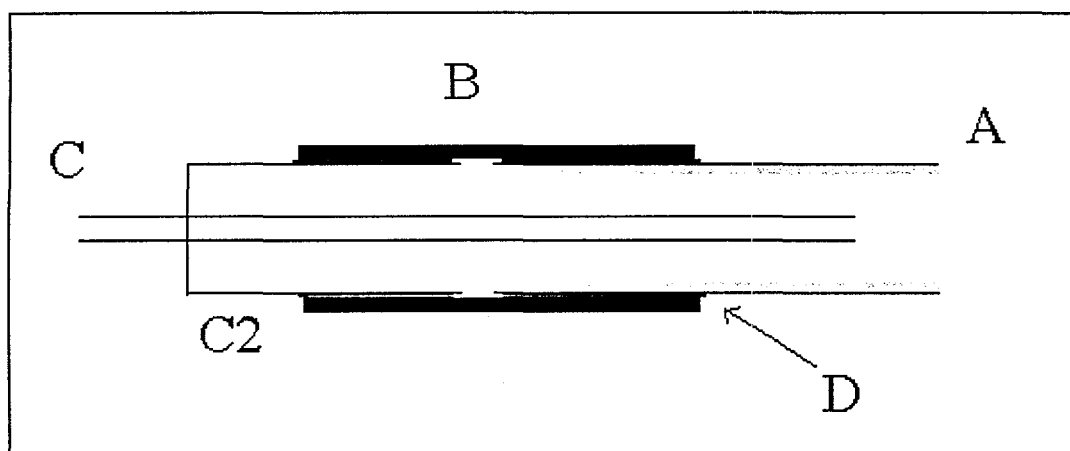
Fig. 1.3. Fitting between reaction tube exit branch and capillary tube.
A: Reaction tube exit flow branch (quartz); B: ceramic fitting tube; C: Capillary tube (steel); C2: transition piece on capillary, also serving as thermal relief; D: teflon tape sealing.

PRESSURE CONTROL

In the new configuration the pressure control strategy has been changed so that the pressure is kept constant by adjusting the exit gas flow (instead of adjusting a 'pressure-sustaining flow' into the pressure vessel). The new control arrangement is illustrated in Fig. 2.1.
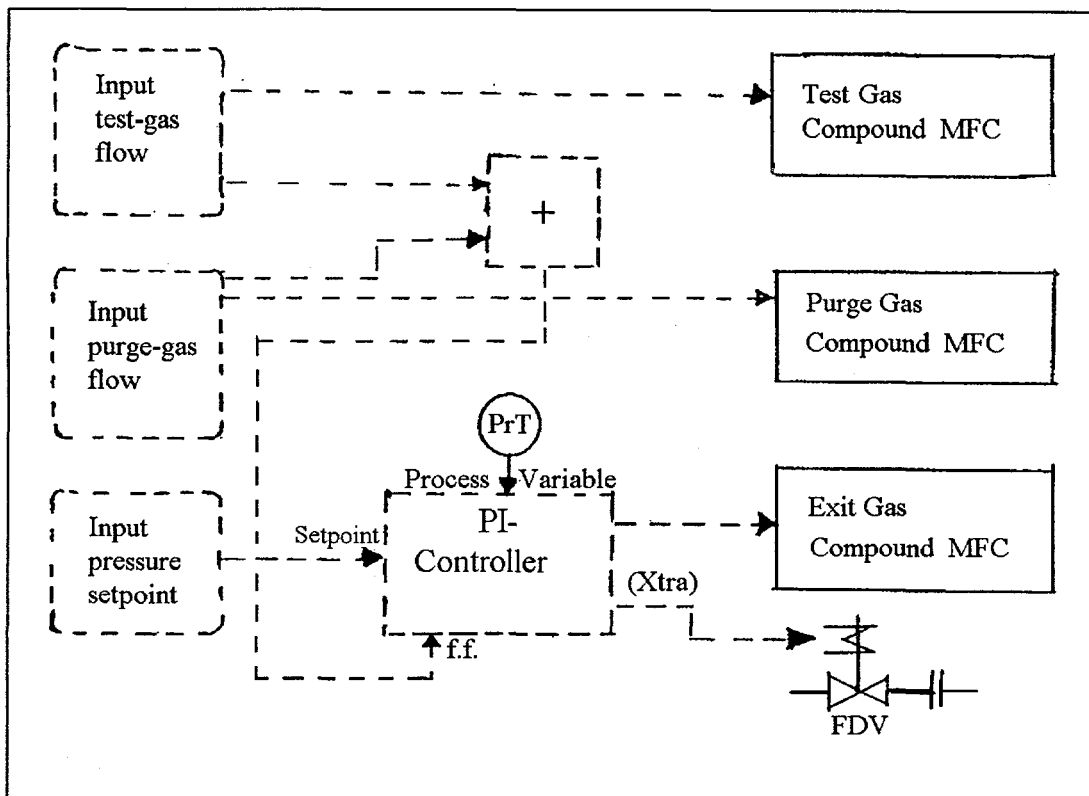
Fig. 2.1. Pressure control arrangement.

For the case that the capacity of the exit gas compound mass-flow controller is not sufficient for the pressure control, this mass-flow controller is supplemented with short-period openings of the fast depressurization solenoid valve FVD to provide extra exit gas flow.

PrT=Pressure transmitter, f.f.=Feed forward.

REFERENCES.

Dobner, S. et al. (1976). *A thermobalance for high pressure process studies.* Thermochimica Acta **16**, pp251-265.

Rathmann, O., Stoholm, P. and Kirkegaard, M.. (1995). *The Pressurized Thermogravimetric Analyzer at the Department of Combustion Research, Risø: Technical Description of the Instrument.* Risø-R-823(EN), Risø National Laboratory, Denmark.

APPENDIX B

PTGA experimental plan for steam gasification

	P_{tot}	PH_2O	PH_2	650	700	750	800	850	875	900	925
Wheat	10	1,5				HH2O#07 HH2O#15	HH2O#05 HH2O#09	HH2O#10		HH2O#32 HH2O#11	
	10	0,75				HH2O#17	HH2O#13	HH2O#12		HH2O#18 HH2O#19	
	10	0,35				HH2O#23	HH2O#22	HH2O#21		HH2O#20	
	10	1,5	0,5				HH2O#27 HH2O#28	HH2O#16		HH2O#29	HH2O#30
	10	1,5	1					HH2O#31	HH2O#35	HH2O#33	HH2O#34
	5	0,75				HH2O#26 HH2O#38	HH2O#24 HH2O#37	HH2O#14 HH2O#36		HH2O#25 HH2O#39	
	5	0,35					HH2O#42	HH2O#40		HH2O#41	
	2	0,35					HH2O#45	HH2O#43 HH2O#44		HH2O#49	
	2	0,15					HH2O#51	HH2O#50		HH2O#52	
	1	0,15					HH2O#47	HH2O#01 HH2O#46		HH2O#48	
Willow	10	1,5			HH2O#54	HH2O#53	HH2O#06 HH2O#55				
Giganteus	10	1,5				HH2O#57	HH2O#56	HH2O#58			
Barley	10	1,5		HH2O#61	HH2O#60	HH2O#62	HH2O#59				

HH2O#X: Char#1   HH2O#X: Char#2

Appendix C

List of inverse reactivities.

Header codes: FF P_{tot}, PH_2O [, PH_2], where FF denotes the fuel: wh=Wheat, wil=Willow, gig=Giganteus, bar=Barley.

Top table

Temp. deg C	wh 10, 1.5, 0 char #1	wh 10, 0.75, 0 char #1	wh 10, 0.35, 0 char #1	wh 10, 1.5, 0.5 char #1	wh 10, 1.5, 1 char #1	wh 5, 0.75, 0 char #1	wh 5, 0.75, 0 char #1	wh 5, 0.35, 0 char #2	wh 2, 0.35, 0 char #2	wh 2, 0.15, 0 char #2	wh 1, 0.15, 0 char 1#, #2	wil 10, 1.5, 0	gig 10, 1.5, 0	bar 10, 1.5, 0
650														5.41E-03
700												2.52E-03		2.17E-02
700														
750	3.88E-03	2.41E-03	2.19E-03			2.86E-03	2.59E-03					1.08E-02	4.77E-03	6.22E-02
750	3.59E-03													
800	1.21E-02	9.08E-03	6.37E-03	1.76E-03		1.16E-02	9.33E-03	7.20E-03	7.73E-03	5.23E-03	5.02E-03	3.44E-02	1.21E-02	1.34E-01
800				2.48E-03								3.30E-02		
850	3.71E-02	2.63E-02	1.68E-02	6.24E-03	2.93E-03	3.65E-02	2.85E-02	2.27E-02	2.39E-02	1.35E-02	1.28E-02		3.84E-02	
850											1.41E-02			
875					5.62E-03									
900	1.01E-01	4.92E-02	3.27E-02	2.05E-02	9.43E-03	7.63E-02	6.56E-02	4.81E-02	5.11E-02	4.16E-02	2.90E-02			
900	9.90E-02													
925				4.29E-02	1.85E-02									
925														

Bottom table

Temp. deg C	wh 10, 1.5, 0 char #1	wh 10, 0.75, 0 char #1	wh 10, 0.35, 0 char #1	wh 10, 1.5, 0.5 char #1	wh 10, 1.5, 1 char #1	wh 5, 0.75, 0 char #1	wh 5, 0.75, 0 char #1	wh 5, 0.35, 0 char #2	wh 2, 0.35, 0 char #2	wh 2, 0.15, 0 char #2	wh 1, 0.15, 0 char 1#, #2	wil 10, 1.5, 0	gig 10, 1.5, 0	bar 10, 1.5, 0
650														1848.4
700												3968.3		460.8
700														
750	2577.3	4149.4	4566.2			3496.5	3861.0					925.9	2096.4	160.8
750	2785.5													
800	826.4	1101.3	1569.9	5681.8		862.1	1071.8	1388.9	1293.7	1912.0	1992.0	290.7	824.4	74.7
800				4032.3								303.0		
850	269.5	380.2	595.2	1602.6	3413.0	274.0	350.9	440.5	418.4	740.7	781.3		260.6	
850											709.2			
875					1779.4									
900	99.0	203.3	305.8	487.8	1060.4	131.1	152.4	207.9	195.7	240.4	344.8			
900	101.0													
925				233.1	540.5									
925														

Appendix D

Fuel analysis

Analyses of the pulverized biomass, wheat straw, barley straw, willow and giganteus (elephant grass) have been performed by dk-TEKNIK, and the results are listed in Table D.1-D.4.

Table D.1. Proximate and ultimate analysis of the pulverized biomass.

	w%				w% (water free basis)			
	Wheat	Barley	Willow	Giganteus	Wheat	Barley	Willow	Giganteus
Water	10.0	12.1	11.1	14.2				
Ash	5.8	2.4	1.9	1.3	6.4	2.7	2.1	1.5
Sulphur	0.15	0.13	0.08	0.09	0.17	0.15	0.10	0.10
Volatile	69.6	70.2	69.9	70.4	77.3	79.9	78.6	82.1
Hydrogen	5.2	5.4	5.9	5.4	5.8	6.14	6.6	6.3
Carbon	42.5	41.5	43.8	41.5	47.2	47.2	49.3	48.4
Nitrogen	0.6	0.7	1.0	0.3	0.7	0.8	1.1	0.3
Chlorine	0.15	0.26	0.029	0.11	0.17	0.30	0.033	0.13
Sodium	0.031	0.048	0.045	0.025	0.034	0.055	0.051	0.029
Potassium	0.63	1.2	0.34	0.35	0.70	1.37	0.38	0.41

Table D.2. Physical properties.

	MJ per kg fuel				MJ per kg water free fuel			
	Wheat	Barley	Willow	Giganteus	Wheat	Barley	Willow	Giganteus
Higher heating value	17.16	16.96	17.92	16.8	19.10	19.2	20.16	19.58
Lower heating value	15.82	15.52	16.4	15.3				
Lower heating value on water free basis					17.85	17.99	18.77	18.24

Table D.3. Ash analysis.

	w% (water free basis)			
	Wheat	Barley	Willow	Giganteus
SiO_2	62	22	15	39
Al_2O_3	1.7	0.64	1.6	1.6
Fe_2O_3	2.0	0.67	0.92	1.1
CaO	8.1	18	32	8.6
MgO	1.8	2.1	3.0	5.9
Na_2O	0.36	1.9	2.6	2.2
K_2O	14	41	17	27
Cl	0.55	4.5	0.11	3.5
CO_2	0.31	6.2	18	0.54
SO_3	2.6	4.3	1.5	4.9
P_2O_5	2.4	4.9	9.3	6.3

The ash analyses listed in Table D.4 were based on ashes produced in the laboratory from unpyrolyzed straw in a reducing atmosphere at 500°C.

Table D.4. Ash fusion temperatures (DS/ISO 540).

	Deformation temperature (°C)	Hemisphere temperature (°C)	Flow temperature (°C)
Wheat	790	1120	1320
Barley	1160	1230	1250
Willow	1110	1470	1500
Giganteus	890	990	1100

Steam Gasification of Wheat Straw, Barley Straw, Willow and Giganteus

Lars K. Hansen, Ole Rathmann, Aksel Olsen and Karin Poulsen

Abstract (max. 2000 characters)

A thorough experimental study of the H_2O gasification char-reactivity of wheat straw, barley straw, willow and giganteus at 1-10 bar total pressure, 0.15-1.5 bar H_2O and 0-1.0 bar H_2 and 750-925 C, was performed in a Pressurized Thermogravimetric Analyzer. There were a total of 58 experiments.

Kinetic experiments with char of wheat straw at 10 bar total pressure showed that the reactivity increases with rising temperature and increasing partial pressure of H_2O, while it decreases with increasing partial pressure of H_2. At constant partial H_2O pressure in the absence of H_2, an indication of a negative influence by the total pressure was observed.

Except for the effect of total pressure, the experimental data were analyzed by means of the Langmuir-Hinshelwood equation, including both inhibition by H_2 and reactivity limitation at high H_2O concentration. Also, the reactivity profile was assumed to be independent of temperature and reactant concentration. The value found for the main activation energy E_1, 149 kJ/mole, describing the temperature dependence at low H_2O concentration, is close to experimental values for biomass reported by other workers. At conditions relevant to both fluid-bed and entrained-flow gasifier types the present results indicate an inhibiting effect of the product gas H_2, reducing the reactivity by a factor of up to 10.

A screening study of steam gasification of barley straw, willow and giganteus in addition to the wheat straw showed reaction rates with rather equal temperature dependence. However, at equal temperatures, there was a spread in reactivity of about 10 times from the lowest (wheat and giganteus) to the highest (barley), probably due to different contents of catalytic elements.

The project has been carried out under the EFP-95 programme for the Danish Ministry of Environment and Energy and for the Danish utility associations Elsam and Elkraft.

Descriptors INIS/EDB